

# NEUROExos: a powered Elbow Orthosis for Post-Stroke Early Neurorehabilitation

Marco Cempini, *Student Member, IEEE*, Francesco Giovacchini, Nicola Vitiello, *Member, IEEE*,  
Mario Cortese, Matteo Moisé, Federico Posteraro, Maria Chiara Carrozza, *Member, IEEE*

**Abstract**— This paper presents the development of a portable version of the robotic elbow exoskeleton NEUROExos, designed for the treatment of stroke survivors in acute/sub-acute phases. The design was improved by a novel Series Elastic Actuation (SEA) system. The system implements two control modalities: a near-zero output impedance torque control and a passive-compliance position control.

**Keywords**— Exoskeleton, Series Elastic Actuator, Neurorehabilitation, Post-stroke, Early Rehabilitation

## I. INTRODUCTION

Stroke is one of the major cause of chronic impairment or disabilities, and post-stroke rehabilitation deeply involves orthopedic and therapeutic medicine, clinical assessment facilities and methodologies, and study of neurological phenomena like neural plasticity [1]-[3]. A long-debated question is on how to increase the probability of a functional recovery, which may be not achieved even after a prolonged rehabilitative treatment. Many studies [2], [4] suggest that the rehabilitation in the early stages following a stroke (namely *early-rehabilitation*, from 1 week to 1 month after the stroke) can promote recovery and improve successful outcomes, even if a quantitative demonstration of such hypothesis has not yet been assessed [5].

Most post-stroke rehabilitation approaches [2]-[3] stressed the fact that movement therapies are largely beneficial if applied for several hours per day. The demand for long and repetitive mobilization session (either in clinical setting or at home) has brought to the issue of providing peculiar medical or healthcare devices. The robot-aided neurorehabilitation is a fast-growing and promising research stream which involves many implications from the clinical, engineering and social points of view [6].

Upper-limb rehabilitation [4] is really important for stroke survivors, since it directly addresses the restoration of functional motion for daily-living activities. During the acute and sub-acute phases, a paretic arm shows a contracted and adducted position [7], with a close elbow and slumped shoulder. Most basic exercises involve mobilization of one single degree of freedom (DoF) at a time, trying to bring

This work was supported in part by the European Union (FP7/2007-2013) within CYBERLEGS (G. A. 287894) and WAY Projects (G. A. 288551); Regione Toscana under the Health Regional Research Programme 2009 within the EARLYREHAB Project, and Italian Government within the AMULOS Project, Industria 2015, G.A. MI01\_00319.

M. Cempini, F. Giovacchini, N. Vitiello, M. Cortese, M. Moisé, and M.C. Carrozza are with The BioRobotics Institute, Scuola Superiore Sant'Anna, viale Rinaldo Piaggio, 34, 56025, Pontedera (PI), Italy.

F. Posteraro is with the Neurorehabilitation Department, Auxilium Vitae Rehabilitation Centre Volterra, USL5 Pisa, Volterra (PI), Italy.

Marco Cempini is corresponding author to provide phone: +39 050 883475; fax: +39 050 883101; e-mail: [m.cempini@sssup.it](mailto:m.cempini@sssup.it).

away the arm from the body: elbow flexion, arm external rotation, shoulder abduction and straight arm flexion. The design of state-of-the-art robotic devices for upper-arm post-stroke rehabilitation does not comply with such conditions [9]-[13]. Among these, a few devices follow an exoskeleton-like approach: standard rehabilitation practices involve a close contact between the therapist and the subject, in order to regulate the motion strength and velocity to the arm condition and to apply countermeasures for subject's compensatory strategies [1]-[2], [7], sudden spasticity [8], or other joint-axis misalignment effects (the most prominent for post-stroke upper arm is the shoulder subluxation, [8]), which can affect the exercise's results. While end-point machines cannot be capable of an adaptive behaviour towards the user's single joints, exoskeletons may provide the capability of controlling their trajectory independently and to comply with the patient's condition, given a proper sensorization and actuation means. Additionally, such a direct interaction may provide quantitative and direct assessment of patient's performances, which may help in planning rehabilitation treatments [2], [6].

In this paper, we tackled the problem of providing a wearable exoskeleton for the mobilization of paretic/spastic elbow condition. The exoskeleton is a revised version of the NEUROExos prototype [14]-[19], a highly-wearable device with joint self-alignment characteristics, developed at The BioRobotics Institute of Scuola Superiore Sant'Anna (Pisa, Italy). This paper presents its actuation, transmission and control systems enhancements: they include a safety clutch and a series elastic actuation (SEA) architecture [20]-[21] with a novel torsional spring element, the latter increasing robot's joint compliance and enabling both position/torque-control methods. The whole platform's deployment has been carefully studied in portability and accessibility, in order to be easily used in compliance with clinical settings.

## II. DESIGN REQUIREMENTS

In the new version of NEUROExos (that we call Elbow Module v1.0) we propose a revised design for the actuation, transmission and control systems.

### A. General Requirements

Peculiar features of NEUROExos are the double shell structure and the 4-DoF passive self-alignment mechanism, [14]. Briefly, the device is composed of two frames, corresponding to human arm and forearm, connected by the actuated hinge joint. Both frames employ a double shell structure, with a structural carbon-fibre made outer shell, and an inner shell, molded in thermoformed plastic and tailored on the wearer's arm, used for a steady but comfortable physical interface. The hinge joint is connected to the upper

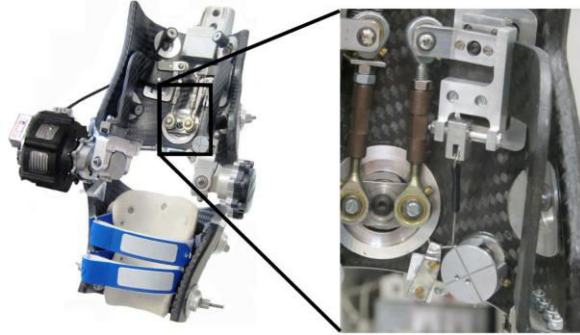


Fig. 1. NEUROExos actuated joint is asymmetric between internal and external side: a spring-loaded cam applies a constant force to counter-balance the asymmetrical load.

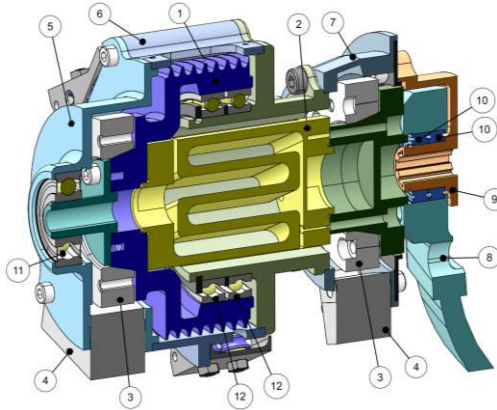


Fig. 2. Cross section of the exoskeleton actuated joint's transmission. (1) Driven pulley. (2) Torsional spring. (3) Absolute encoder ring. (4) Absolute encoder readhead. (5)-(7) Covers. (8) Exoskeleton lower frame connection. (9). Exoskeleton upper frame connection. (10)-(12) Ball bearings.

frame through a closed-chain mechanism, composed by 13 passive joints, resulting into a 4-DoF passive mechanism, so that the powered axis has the same degree of laxity of -and automatically aligns to- the human elbow's one [14]-[17], [22]-[24]. Passive joints also tolerate intra- and inter-subject variability in elbow axis orientation and position.

#### B. Actuation and control strategy

The NEUROExos Elbow Module v1.0 employs a SEA [20]. Such configuration has been chosen accordingly to the following considerations. The exoskeleton control system should provide at least two different therapy protocols, in order to achieve basic physical rehabilitation exercises, namely *robot-in-charge* and *patient-in-charge* [22], [25]. In robot-in-charge mode, which is best suited for the initial stage of the rehabilitation process when patients cannot move autonomously, the robot promotes a desired motion pattern and has a relatively high joint impedance. Patient-in-charge mode is needed when the subject can control some movements of his/her limb, and requires some assistance from the system to complete the task. In this latter case, the robot should not hinder the patient motion, but rather it should show near-zero impedance while assisting the user. SEAs allow the implementation of both high- and near-zero joint impedance control strategies, as presented in [22].

In order to mobilize elbow joints affected by spasticity, NEUROExos can supply a maximum joint torque of 30

N·m. The SEA spring stiffness was set to  $100 \text{ N}\cdot\text{m}\cdot\text{rad}^{-1}$ , which is a value comparable with the one of human elbow [26], and thus prevents the subject from an uncomfortable (or even painful) interaction with an excessively stiff device in case of involuntary spastic motions.

#### D. Support frame

Targeted patients, because of their motor disorders, can be forced on a wheelchair or, in case of acute strokes, in bed. From practical and usability consideration, it arises the need for the exoskeleton to be supported on a structure easily movable in a clinical environment; furthermore such structure must allow adjustment of the exoskeleton spatial configuration in order to meet the specific patient's conditions.

### III. SYSTEM DESIGN AND PERFORMANCE

The NEUROExos Elbow Module v1.0 is constituted by three main parts, meeting the aforementioned requirements: the exoskeleton module, the remote actuation/control system, and a moveable stand that carries all of the mentioned modules.

#### A. Exoskeleton joint design

The mechanical power is transmitted from the remote actuation unit to the exoskeleton through a pair of Bowden cables routing steel wire ropes (Carl Stahl® U8191517), by means of a Capstan configuration. The driven pulley belongs to the transmission torque unit on the external lateral side of the exoskeleton actuated joint, and transmits the motor torque to the elbow joint shaft through a custom made torsional spring (see Fig. 1 and Fig. 2). Since the driven pulley lays on the external lateral side of the exoskeleton, its weight loads asymmetrically the 4-DoF passive mechanism. Asymmetrical load is then partially counter-balanced by a spring-loaded cam mechanism (see Fig. 1). The driven pulley and its external frame are built in lightweight materials, i.e., Ergal and Tecatron™ GF40 respectively.

Two 32-bit absolute encoders (Renishaw® RESOLUTE™, ring: RESA30USA052B, readhead: RA32BAA052B30F) provide a measure of the spring deformation, and – being known the spring stiffness – of the torque applied to the joint. The use of absolute encoders allows easy initialization of the control system, contrarily to the incremental optical encoders that require to be initialized to a predefined value.

#### B. Torsional spring

The general goal in designing was weight and encumbrance reduction; however, the pulley's diameter is related to the maximum desired torque ( $30 \text{ N}\cdot\text{m}$ ) through the admitted tension crossing the cables, and so cannot be arbitrary small. To comply with the cable fatigue-limit tension, a diameter of 75 mm was chosen. This feature affects the constraints over the torsional spring's shape: to limit the encumbrance, we enclosed the spring into the pulley assembly, together with a ball-bearing set mounting (Fig. 2). A literature review over torsional spring suggested that "flat" designs, such as [25], [27], were not well suited for our assembly. We opted for a shaft-like element, enclosed in a straight cylinder, transmitting the torque between two parallel flanges.

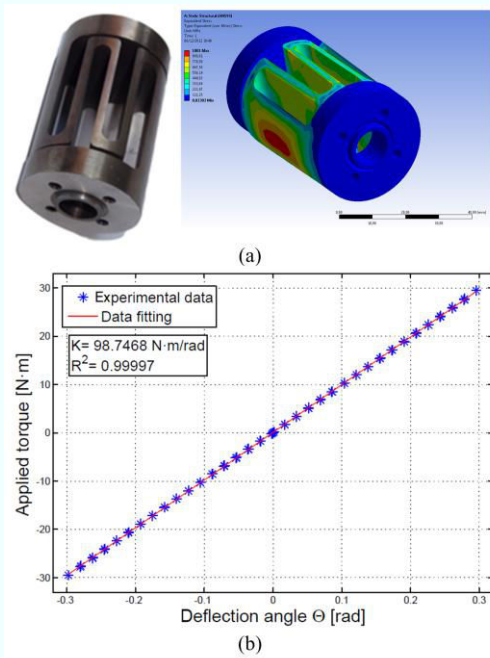


Fig. 3. Torsional Spring. (a) Overview of the component and FEM simulation results under a load of 30 N·m. (b) Torque vs. deflection characterization, and the linear interpolator.

For the elastic part's sizing, we started from a straight plate assumptions, folded in a S-profile and fitted into the outer cylinder (see Fig. 3). An iterative FEM simulation process led to the tuning of the detailed dimensions set, till the final shape. As optimization objective, the maximum von Mises stress ( $\sigma_{VM}$ ) had to be less than 1000 MPa, with an applied torque  $T$  of 30 N·m, and the torsional stiffness  $K$  to be around  $100 \text{ N·m·rad}^{-1}$ . The chosen material is a Maraging steel (Böhler W720, Young's modulus of 193 GPa, yield stress of 1815 MPa): final simulation results are  $\sigma_{VM} = 1001 \text{ MPa}$  (hence a safety factor of 1.8 over elastic limit) and a stiffness  $K_{FEM} = 110 \text{ N·m·rad}^{-1}$ , corresponding to a relative rotation of the spring's flanges of  $16^\circ$ . Final dimensions are 35 mm outer diameter and an overall length of 55.2 mm.

The choice of the depicted shape for the torsional element was also driven from consideration over its manufacturability. Our spring is obtained from a turned cylindrical workpiece, then the central S-profile is cut out through a wire electrical discharge machining (WEDM) process, along a simple path (straight and circular segments): the easiness of the working process guarantees a high reliability in the final component. After the cutting process, the spring underwent to an annealing treatment ( $820^\circ\text{C}/1\text{h}/\text{air}$ ), in order to avoid thermal modification of the structure due to the WEDM, then to an ageing treatment ( $480^\circ\text{C}/3\text{h}/\text{air}$ ) to guarantee the nominal yield stress value.

Torque vs. deflection behaviour of the spring was characterized experimentally by using actuated joint assembly as setup. The torque was applied by a cable wrapped on the pulley and pulled by a tensile/compression test machine (Instron® 4464 load frame). The spring rotational deflection was measured by an encoder (same typology as depicted in III.A) while torque was derived from the Instron's force reading (see Fig. 3). The experimental stiffness  $K$  is around 10% lower than the FEM predicted one

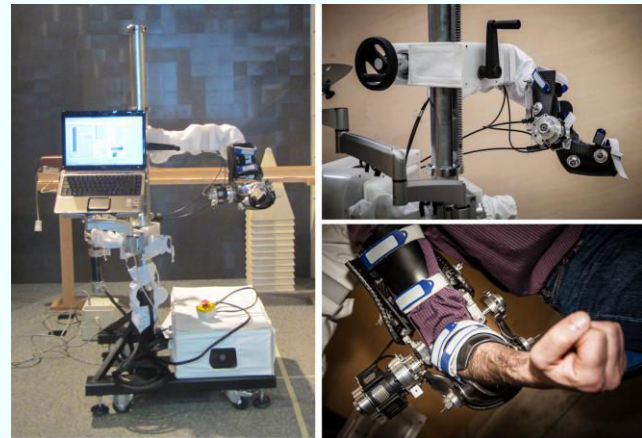


Fig. 4. Overview of the Elbow Module v1.0. Laptop swivel arm, controller and power supply box, adjustable exoskeleton support are visible.

( $K = 98.75 \text{ N·m·rad}^{-1}$ ): this is still a better prediction than other similar results in literature, [27]). The behavior is well approximated by a linear interpolator ( $R^2=0.99997$ ).

### C. Remote actuation/control unit and stand support

Carried on a dedicated adjustable appendix of the moveable stand support (see Fig. 4), the motor unit is composed of a DC servomotor (Maxon® EC motor EC60, 400W), an Harmonic Drive reduction stage (Harmonic Drive® CPL-17A-080-2) with a reduction ratio of 80, a grooved pulley which the steel cables wrap around. A safety clutch (R+W® SK1/15/D/20) is inserted between the gear output shaft and the pulley, so that if the gearmotor exerts a torque higher than a threshold value (settable between 35 N·m and 70 N·m), the transmission is decoupled without hurting the wearer. A system for manual adjustment of the steel cables' pretension is provided, by means of lead-screws which regulate the Bowden hoses' path from the motor unit to the exoskeleton. The exoskeleton is hung on an adjustable spherical joint at the tip of a liftable and extendible support. The weight of the entire structure is around 35 Kg.

A plastic box contains the control electronics (NI sbRIO-9632, Austin, Texas), which runs the real-time control system, the Maxon EPOS2 velocity servos, and a custom PCB to route the wires from/to the motor unit and all sensors. NEUROExos implements two control strategies (block diagrams are reported in Fig. 5). Fig. 6 shows the position control performance in a prototypical robot-in-charge task where the device is programmed to displace the elbow joint of a healthy subject along a sinusoidal 0.5-Hz trajectory [14]. Fig. 7 shows the performance of the torque control when an healthy subject displaces the NEUROExos joint, being the desired torque equal to zero, thus simulating a typical patient-in-charge task. Over a frequency range of 0.3-1.5 Hz, the parasitic stiffness ranges from 1 to  $10 \text{ N·m·rad}^{-1}$ , similar to what was found in [14].

## IV. CONCLUSION

We presented new joint, actuation unit, and preliminary experimental results of the control strategies of NEUROExos. Future works will aim at carrying out a deeper experimental characterization and validation in a clinical setting with patients affected by neurological disorders.

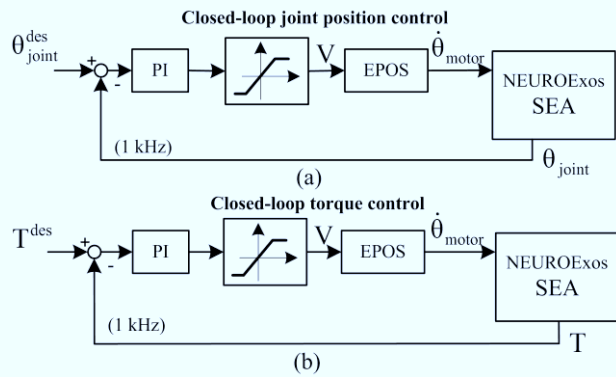


Fig. 5. Control strategies. a) Joint position control. b) Torque control.  $V$  is the voltage signal to command the EPOS2 driver. The joint torque  $T$  is estimated by measuring the torsional spring deflection.

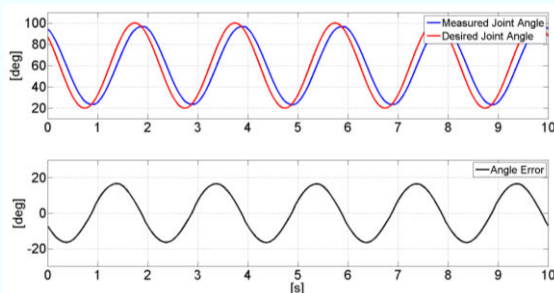


Fig. 6. Position control: 0.5-Hz sine wave. Top) Measured vs. desired joint position. Down) Angular error. Data show an amplitude attenuation of -0.83 dB, and a phase lead of 23°.

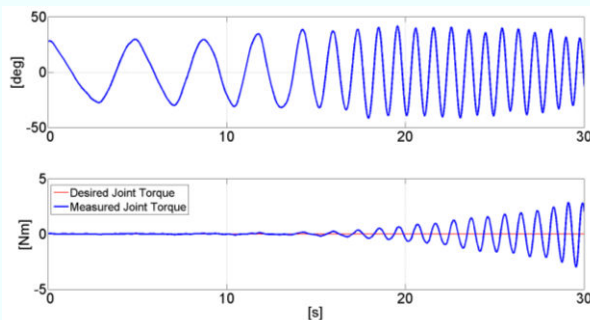


Fig. 7. Torque control. Top) Joint displacement. Down) Desired vs. measured joint torque. Parasitic torque increases up to 2.75 N·m, when the joint angle varies between  $\pm 35^\circ$  with a frequency of 1.3 Hz.

## REFERENCES

- [1] E. Taub, G. Uswatte, and T. Elbert, "New treatments in neurorehabilitation founded on basic research", *Nat. Rev. Neurosci.*, vol. 3, no. 3, pp. 228-236, 2002.
- [2] P. Langhorne, J. Bernhardt, and G. Kwakkel, "Stroke Rehabilitation", *The Lancet*, vol. 377, no. 9778, pp. 1693-1702, 2011.
- [3] J.W. Krakauer, "Motor learning: its relevance to stroke recovery and neurorehabilitation", *Cur. Op. in Neur.*, vol. 19, no.1, pp. 84-90, 2006.
- [4] G. Prange, M. Jannink, C. Groothuis-Oudshoorn, H. Hermens, and M. Ijzerman, "Systematic review of the effect of robot-aided therapy on recovery of the hemiparetic arm after stroke", *J. of Rehab. Res. and Dev.*, vol. 43, no. 2, pp. 171-184, 2006.
- [5] Bernhardt J, Thuy M.N., Collier J.M., Legg L.A., "Very early versus delayed mobilisation after stroke", *Stroke*, vol. 40, no. 1, pp. 489-490, 2009.
- [6] H.I. Krebs, N. Hogan, M.L. Aisen and R.B.T. Volpe, "Robot-aided Neurorehabilitation", *IEEE Trans. on Rehab. Eng.*, vol. 6, no. 1, pp. 75-87, 1998.
- [7] D.G. Liebermann, M.F. Levin, S. Berman, H.P. Weingarden, P.L. Weiss, "Kinematic features of arm and trunk movements in stroke patients and age-matched healthy controls during reaching in virtual

- and physical environments", in *Proc. of the IEEE Int. Conf. Virt. Rehab.*, pp. 179-184, 2009.
- [8] R.D. Zorowitz, M.B. Hughes, D. Idank, T. Ikai, M.V. Johnston, "Shoulder pain and subluxation after stroke: correlation or coincidence?", *Am. J. Occup. Ther.*, vol. 50, no. 3, pp. 194-201, 1996.
- [9] T. Nef, M. Mihelj, and R. Riener, "ARMin: A robot for patient-cooperative arm therapy", *Med. Biol. Eng. Comput.*, vol. 45, no. 9, pp. 887-900, 2007.
- [10] S.J. Ball, I.E. Brown, and S.H. Scott, "MEDARM: a rehabilitation robot with 5DOF at the shoulder complex", in *Proc. of IEEE/ASME Int. Conf. on Adv. Intell. Mech.*, pp. 1-6, 2007.
- [11] G. Rosati, P. Gallina, S. Masiero, A. Rossi, "Design of a new 5 d.o.f. wire-based robot for rehabilitation," in *Proc. of IEEE Int. Conf. on Reh. Rob. (ICORR)*, Chicago, US, pp. 430-433, 2005.
- [12] W.M. Nunes, L.A.O. Rodrigues, L.P. Oliveira, J.F. Ribeiro, J.C.M. Carvalho, R.S. Goncalves, "Cable-based parallel manipulator for rehabilitation of shoulder and elbow movements", in *Proc. of IEEE Int. Conf. on Reh. Rob. (ICORR)*, Zurich, Switzerland, pp. 1-6, 2011.
- [13] J. Klein, S. Spencer, J. Allington, J.E. Bobrow, D.J. Reinkensmeyer, "Optimization of a Parallel Shoulder Mechanism to Achieve a High-Force, Low-Mass, Robotic-Arm Exoskeleton," *IEEE Trans. On Rob.* vol. 26, no. 4, pp.710-715, 2010.
- [14] N. Vitiello, T. Lenzi, S. Roccella, et al., "NEUROExos: A Powered Elbow Exoskeleton for Physical Rehabilitation", *IEEE Trans. on Rob.*, vol. 29, no. 1, pp. 220-235, 2013.
- [15] T. Lenzi, N. Vitiello, S.M.M. De Rossi, S. Roccella, F. Vecchi, and M.C. Carrozza, "NEUROExos: a variable impedance powered elbow exoskeleton", in *Proc. of the IEEE Int. Conf. on Rob. and Aut. (ICRA)*, Shanghai, China, pp. 1419-1426, 2011.
- [16] T. Lenzi, S.M.M. De Rossi, N. Vitiello, and M.C.C. Carrozza, "Intention-Based EMG Control for Powered Exoskeletons", *IEEE Trans. on Biomed. Eng.*, vol. 59(8), pp. 2180- 2190, 2012.
- [17] R. Ronsse, N. Vitiello, T. Lenzi, J. Van den Kieboom, M.C. Carrozza, and A.J. Ijspeert, "Human-robot synchrony: flexible assistance using adaptive oscillators", *IEEE Trans. on Biomed. Eng.*, vol. 58(4), pp. 1001-1012, 2011.
- [18] T. Lenzi, N. Vitiello, S.M.M. De Rossi, A. Persichetti, F. Giovacchini, S. Roccella, F. Vecchi, M.C. Carrozza, "Measuring Human-Robot Interaction on Wearable Robots: a Distributed approach", *Mechatronics*, vol. 21(6), pp. 1123-1131, 2011.
- [19] M. Donati, N. Vitiello, S.M.M. De Rossi, T. Lenzi, S. Crea, A. Persichetti, F. Giovacchini, B. Koopman, J. Podobnik, M. Munihi, M.C. Carrozza, "A Flexible Sensor Technology for the Distributed Measurement of Interaction Pressure", *Sensors*, vol. 13, pp. 1021-1045, 2013.
- [20] G. Pratt and M. M. Williamson, "Series elastic actuators," in *Proc. IEEE Int. Conf. Intell. Robots Syst.*, Pittsburgh, PA, 1995, pp. 339-406.
- [21] N. Vitiello, T. Lenzi, S. M. M. De Rossi, S. Roccella, and M. C. Carrozza, "A sensorless torque control for Antagonistic Driven Compliant Joints," *Mechatronics*, vol. 20, no. 3, pp. 355-367, 2010.
- [22] A. H. A. Stienen, E. E. G. Hekman, H. ter Braak, A.M. Aalsma, F.C. van der Helm, H. van der Kooij, "Design of a rotational hydro-elastic actuator for a powered exoskeleton for upper-limb rehabilitation," *IEEE Trans. Biomed. Eng.*, vol. 57, no. 3, pp. 728-735, Mar. 2010.
- [23] M. Cempini, S.M.M. De Rossi, T. Lenzi, N. Vitiello, M.C. Carrozza, "Self-Alignment Mechanisms for Assistive Wearable Robots: A Kinetostatic Compatibility Method", *IEEE Trans. on Rob.*, vol. 29, no. 1, pp. 236-250, 2013.
- [24] A. Chiri, N. Vitiello, F. Giovacchini, S. Roccella, F. Vecchi, and M. C. Carrozza, "Mechatronic design and characterization of the index finger module of a hand exoskeleton for post-stroke rehabilitation," *IEEE/ASME Trans. Mech.*, vol. 17, no. 5, pp. 884-894, 2012.
- [25] J. F. Veneman, R. Ekkelenkamp, R. Kruidhof, et al., "A series elastic- and Bowden-cable-based actuation of use torque actuator in exoskeleton-type robots," *Int. J. Robot. Res.*, vol. 25, no. 3, pp. 261-281, 2006.
- [26] M. O. Abe and N. Yamada, "Modulation of elbow joint stiffness in a vertical plane during cyclic movement at lower or higher frequencies than natural frequency," *Exp. Brain Res.*, vol. 153, pp. 394-299, 2003.
- [27] F. Sergi, D. Accoto, G. Carpino, N.L. Tagliamonte, E. Guglielmelli, "Design and Characterization of a Compact Rotary Series Elastic Actuator for Knee Assistance During Overground Walking", in *Proc. IEEE Int. Conf. on Biomed. Rob. and Biomech.*, pp. 1931-1936, 2012.